Reactive and Functional Polymers 221 (2026) 106652

Contents lists available at ScienceDirect

Reactive and Functional Polymers

journal homepage: www.elsevier.com/locate/react

Synthesis and characterization of biomimetic hybrid membranes based on a side chain liquid crystalline poly(2-oxazoline) for selective proton transport

Jordi Guardià [a], Krzysztof Artur Bogdanowicz [b,*], José Antonio Reina [a], Marta Giamberini [c], Agnieszka Iwan [d], Xavier Montané [a,*]

[a] Universitat Rovira i Virgili, Department of Analytical Chemistry and Organic Chemistry, C/Marcel·lí Domingo 1, 43007 Tarragona, Spain
[b] Military Institute of Engineer Technology, Obornicka 136, 50-961 Wrocław, Poland
[c] Universitat Rovira i Virgili, Department of Chemical Engineering, Av. Països Catalans 26, 43007 Tarragona, Spain
[d] Faculty of Security and Safety Research, General Tadeusz Kosciuszko Military University of Land Forces, Czajkowskiego 109, 51-147 Wrocław, Poland

ARTICLE INFO

Keywords:
Side chain liquid crystalline poly(2-oxazoline)
Biomimetic membranes
Selective transport
Proton transport
Fuel cells

ABSTRACT

Designing biomimetic membranes with controlled and selective ion transport pathways is essential for next-generation electrochemical and energy-conversion systems. In this work, the cation transport properties of hybrid membranes composed of a side chain liquid crystalline poly(2-oxazoline), poly(2-(3,4,5-tris(4-dodecyloxybenzyloxy)phenyl)-2-oxazoline (PTOx40), supported on a polyester fabric were investigated. Polymer columns were homeotropically oriented by thermal treatment. X-ray diffraction revealed that hydrophobic substrates (fluorinated ethylene propylene resin and silanized glass) promoted better homeotropic orientation of the polymer columns than hydrophilic substrates (untreated glass). Wettability studies indicated comparable absorption behaviour for water and methanol in all membranes. Methanol uptake was consistently lower than that of water, highlighting their suitability for methanol-based hydrogen systems. Compared with Nafion® 117, these PTOx40-based membranes exhibited superior dimensional stability and a hydrophobic character. Cation transport was examined through electrochemical impedance spectroscopy (EIS), permeability tests, and linear sweep voltammetry (LSV). Although EIS confirmed the non-ionic nature of these membranes, LSV measurements demonstrated that oriented membranes exhibited lower resistance densities than unoriented ones. This strong dependence on column alignment underscores the role of columnar self-assembly in facilitating selective ion transport. The PTOx40-based membranes exhibited lower absolute conductivity than Nafion® 117. However, they showed remarkable proton selectivity, highlighting their potential for proton-transfer applications in artificial photosynthesis and sustainable energy technologies.

1. Introduction

Nowadays, the climate change is a reality. The increasing amount of greenhouse gases (GHG) released over the years into the atmosphere for the last century, has led to an increase in the global temperature [1]. To reduce the negative effects of using conventional fuels, the scientific community focuses on developing alternative energy sources to fossil fuels. One such alternative is the proton exchange membrane fuel cell (PEMFC). PEMFC is assembled similarly to a sandwich, with the polymer electrolyte membrane (PEM), in the center, surrounded by two electrodes, one on each side [2]. In the last decades, the importance of PEMFC has risen, especially for power-generating portable devices and automotive applications, due to their low cost, lightweight design, low emissions, and high-power density [3].

Nowadays, PEMFC membranes are based on commercially available perfluorosulfonic acid ionomer (PFSI), like Nafion® 117. However, these types of membranes present some drawbacks. They exhibit poor chemical stability at high temperatures, methanol crossover during operation in direct methanol fuel cells (DMFCs), and a strong dependence on water content in their structure, which limits their operating temperature range to 0–100 °C [4].

Despite the fact that PFSI-based membranes present advantages like excellent proton conductivity and electrochemical stability, alternative materials have been investigated in recent years. For instance, Wang and co-workers reported the use of amino acid-modified chitosan nanofibers to fabricate nanocomposites for proton exchange membranes. These

* Corresponding authors.
E-mail addresses: bogdanowicz@witi.wroc.pl (K.A. Bogdanowicz), xavier.montane@urv.cat (X. Montané).

https://doi.org/10.1016/j.reactfunctpolym.2026.106652
Received 7 November 2025; Received in revised form 24 December 2025; Accepted 13 January 2026
Available online 14 January 2026

nanocomposites achieved good conductivity at 80 °C (0.192 S/cm) and lower methanol crossover compared to typical PFSI-based membranes [5].

A family of polymers that has been extensively investigated because of their wide range of applications – including optoelectronic devices [6], sensors [7], and membranes [8–10], among others – are side chain liquid crystalline polymers (SCLCP)s. Over the past few decades, our research group has focused on the design of different (SCLCP)s for use in ion transport applications as alternatives to Nafion® 117 [11]. By grafting a tapered dendron, 3,4,5-tris[4-(n-dodecan-1-yloxy)benzyloxy] benzoic acid (TAP), onto polyethers or polyamines, dendronized SCLC polyethers and polyamines capable of self-assembling into columnar structures were synthesized [12–15]. This self-assembly process is driven by the π-π stacking interactions among the aromatic moieties of the TAP side dendrons [16]. The resulting columnar structures facilitates the formation of ion-conducting channels through the presence of heteroatoms (oxygen or nitrogen) in the polymer backbone, which define the permeation pathways. Moreover, the dodecyl aliphatic chains impart sufficient column mobility, enabling thermally induced rearrangement and promoting an ideally homeotropic columnar orientation [17]. Notably, self-supported membranes prepared from dendronized SCLC polyethers and polyamines exhibited proton conductivities comparable to that of Nafion® 117 [13,18]. However, most of the synthesized polymers had poor mechanical properties, rendering the resulting membranes fragile and brittle, and therefore requiring a supporting material. The use of this support is expected to reduce brittleness and improve the mechanical properties of the resulting membranes. For instance, Bogdanowicz and *co*-workers embedded SCLC polyamines within anodized aluminium oxide (AAO) discs to prepare hybrid membranes with enhanced mechanical strength. These membranes exhibited good proton conductivity, high permselectivity toward protons over other monovalent cations, and a methanol crossover nearly two orders of magnitude lower than that of Nafion® 117 [19,20].

In a previous published work, we reported the synthesis and characterization of a family of poly(2-(3,4,5-tris(4-dodecyloxybenzyloxy) phenyl)-2-oxazoline) (PTOx) via "living" polymerization, with degrees of polymerization (DP) ranging from 20 to 60 [21]. Owing to the nitrogen atoms present in the polymer backbone, PTOx have the potential to serve as promising materials for preparing membranes capable of ion transport. PTOx40 (DP = 40) was selected for membrane preparation, as it was the only polymer that exhibited a clear hexagonal columnar mesophase, with well-defined clearing and anisotropy temperatures observed after first heating. Furthermore, PTOx40 was incorporated into a polyester fabric support, since self-supported membranes based on this SCLC poly(2-oxazoline) could not be obtained.

In this work, we present the preparation and characterization of hybrid membranes based on a SCLC poly(2-oxazoline), PTOx40, and a polyester fabric support. Furthermore, a comprehensive analysis was performed to evaluate the orientation of the biomimetic polymer channels within the polyester support, the hydrophobic/hydrophilic character of the resulting membranes, and their ionic transport properties. This analysis aimed to assess their potential as ion-conducting materials.

2. Experimental section

2.1. Materials

2-(3,4,5-tris(4-dodecyloxybenzyloxy)phenyl)-4,5-dihydro-1,3-oxazole (TAPOx) was synthesized following the procedure reported by Guardià et al. [21]. Methyl trifluoromethanesulfonate (MeOTf, ≥98%) was supplied by Sigma Aldrich. Morpholine (99%) was purchased from Alfa Aesar. Chlorotrimethylsilane (98%) was supplied by Across Organics, while chlorobenzene was supplied by Scharlab. Tetrahydrofuran (THF) was purchased from Fisher Scientific, and acetone was supplied by SGL (Suministros Generales para Laboratorio, S. L.). Furthermore, chlorobenzene and morpholine were dried prior to use according to literature [22]. The used polyester fabric was Hollytex® (22 g/cm^2).

The following supports were used during the preparation of the hybrid membranes:

- Untreated glass (UG).
- Silanized glass (SG): glass plates were immersed in a 10% (*v*/v) solution of clorotrimethylsilane overnight. After that, hydrophobic glass plates were washed several times with acetone and air-dried overnight.
- Fluorinated Ethylene Propylene Resin (FEPR) sheet, with a thickness of 0.1 mm, was purchased from Saint-Gobain. The FEPR sheet was washed with acetone and air-dried before used.

For membrane assembly and all characterization experiments involving water, Milli-Q ultrapure water was used.

2.2. Synthesis of poly(2-(3,4,5-tris(4-dodecyloxybenzyloxy)phenyl)2-oxazoline) (PTOx40)

Poly(2-(3,4,5-tris(4-dodecyloxybenzyloxy)phenyl)-2-oxazoline) with a degree of polymerization of 40 (PTOx40, Fig. 1) was synthetized by "living" polymerization of TAPOx monomer, as described in a previously published article [21]. The chemical characterization (NMR, FT-IR, degree of polymerization and molecular weight distribution) of PTOx40 is presented in a previous work [21]. $Đ$ (dispersity): 1.16 (Estimated by SEC).

2.3. Membrane preparation

The immersion precipitation process was used to assembly the membranes. This process included the following steps: a 30% solution (*w*/w) of PTOx40 (50 mg) in THF was prepared and cast over the polyester fabric. The hybrid membranes constituted by the polyester fabric and PTOx40 was placed over a support (untreated glass plate, silanized glass plate or FEPR sheet). Later, the impregnated support was immersed in a bath of Milli-Q ultra-pure water for 15 min. Finally, the assembled membranes were air-dried overnight.

After that, a thermal treatment (baking process) was used to homeotropically orient the membranes. In this process, an assembled membrane was placed on a Linkam TP92 hot stage, heated above the polymer clearing temperature (150 °C for these membranes) and kept for 30 min at this temperature. Next, it was slowly cooled down (0.5 °C/min) to the selected annealing temperature (69 or 73 °C). These hybrid membranes were annealed for 24 h. Finally, the hybrid membranes were cooled to RT (Room temperature = 25 ± 5 °C) at 0.5 °C/min. Both processes, the assembly of the membranes and the baking process, are illustrated in Scheme 1. The prepared membranes had a thickness of 220 ± 10 μm.

The membranes obtained were named according to the annealing temperature and the support used in their preparation. In general, the nomenclature used was PTOxM-X-Y, where X denotes the annealing temperature (°C) and Y the abbreviation of the support. The abbreviations for the supports used were UG for untreated glass, SG for silanized glass, and FEPR for the Fluorinated Ethylene Propylene Resin sheet. For example, the code PTOxM-73-UG refers to the membrane annealed at 73 °C using untreated glass as the support.

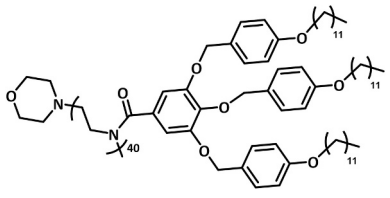

Fig. 1. Chemical structure of PTOx40.

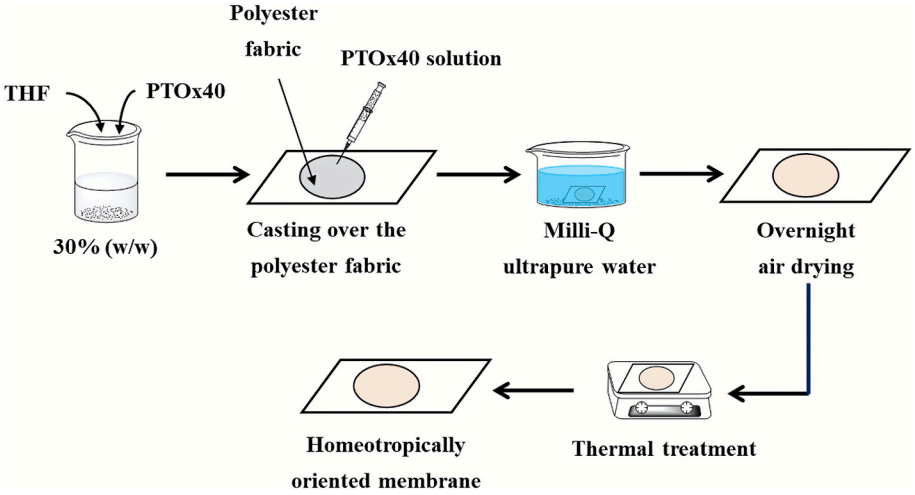

Scheme 1. Procedure used to assemble and achieve homeotropic orientation of hybrid membranes based on PTOx40.

2.4. Characterization techniques

Molecular weight analysis was performed via size exclusion chromatography (SEC) using an Agilent 1200 series system equipped with three serial columns (PLgel 3 μm MIXED-E, 5 μm PLgel MIXED-D and PLgel 20 μm MIXED-A from Polymer Laboratories) and an Agilent 1100 series refractive index detector working at 35 °C. The nominal flow rate was 1.0 mL/min with a sample concentration of 0.1% *w*/w in tetrahydrofuran (THF) as the solvent. The SEC system was calibrated using narrow polystyrene standards from Polymer Laboratories with molecular weights ranging from 500 to 400.000 Da.

Calorimetric analyses were carried out on a Mettler DSC-821 instruments calibrated using indium (156.6 °C) and zinc (419.6 °C) pearls. Samples were placed in an aluminium standard crucible of 40 μL with pierced lids (between 4 and 6 mg of the sample), which were analysed in N_2 atmosphere (gas flow rate of 50 cm^3/min). Heating and cooling rate of 10 °C/min was always employed.

The static contact angles (CA) with water on a membrane surface were measured with an optical goniometer (Ossila LTd, Sheffield, UK) supported by dedicated software. For the tests, water drops of 7 μL were deposited in the sample surface. The contact angle was calculated, immediately after placing the water drop, using the tangent to the surface at the point of contact of three phases, i.e., solid, liquid and gas. For each test reported, at least three drops of water were used.

X-ray diffraction (XRD) measurements were made using a Bruker-AXS D8-Discover diffractometer equipped with a parallel incident beam (Göbel mirror), vertical θ-θ goniometer, XYZ motorized stage and a GADDS (General Area Detector Diffraction System). Samples were placed directly on the Si(510) sample holder for reflection analysis. An X-ray collimator system close-to-the-sample allows to analyse areas of 500 μm. An X-ray diffractometer was operated at 40 kV and 40 mA to generate $Cu_{K\alpha}$ radiation. The GADDS detector was a VÅNTEC-500 (silicon strip technology) placed at 30 cm from the sample. The collected *frame* (2D XRD pattern) covered a 2θ range from 0.9 up to 11°. The exposition time was 600 s per *frame*. Azimuthal scan was performed within the range between 180° and 360°, due to the limitations of the equipment software. In this sense, 180° were considered as 0°, 360° as 180°, with 270° corresponding to 90°. XRD experiments were performed on both sides of the membranes and no differences were detected.

Electrochemical impedance spectroscopy (EIS) analyses were performed using PGStat Autolab M204 (Metrohm Nederland, Barendrecht, Netherlands) coupled to a frequency response analyser (FRA) and two-point cell composed of two copper plates. Membranes with a diameter of 0.8 cm were used. EIS analyses of dry membranes were conducted using a through-plane set-up. The measurements were performed at RT.

Permeability tests were performed using a methacrylate test cell that consisted of two compartments, separated by the tested membrane, containing the feed and the stripping solutions, respectively. The volumes of the feed and the stripping solutions were 200 mL, and the effective membrane area was 0.28 cm^2. For proton transport experiments, the initial concentrations of the feed and stripping solutions was 0.1 M $HCl_{(aq)}$ and 0.1 $M_{(aq)}$ of: NaCl, LiCl or KCl, respectively. The pH of the stripping solution was measured every 10 s using a pH-conductivity meter CPC-505 connected to a computer, which recorded the results. All experiments were performed in triplicate.

Linear sweep voltammetry (LSV) tests were performed using Metrohm / Eco Chemie Autolab PGSTAT12 (Metrohm, Barendrecht, Netherlands) in potentiostatic mode with current ranging (automatic) from 100 mA to 100 nA, potential range from 0 V to 5 V, step 0.01 V, and scan rate 0.01 V/s. The experimental setup is presented in Fig. 2. The distance between the reference electrodes (Ag/AgCl) and the membrane was 1 cm. The solution volume in each compartment was 200 mL. The measurements were performed at RT. Samples for these experiments were placed in a Teflon sheet with a hole in the middle, giving a total membrane area equal to 0.28 cm^2. 0.1 M $HCl_{(aq)}$ solution was used to study proton transport. Additionally, measurements with solutions of 0.1 $M_{(aq)}$ containing distinct chloride salts (LiCl, KCl and NaCl) were performed to study the selectivity of the membranes.

For the solution uptake tests, weighted membranes were immersed in Milli-Q ultrapure water at RT. Wet membranes were weighted every

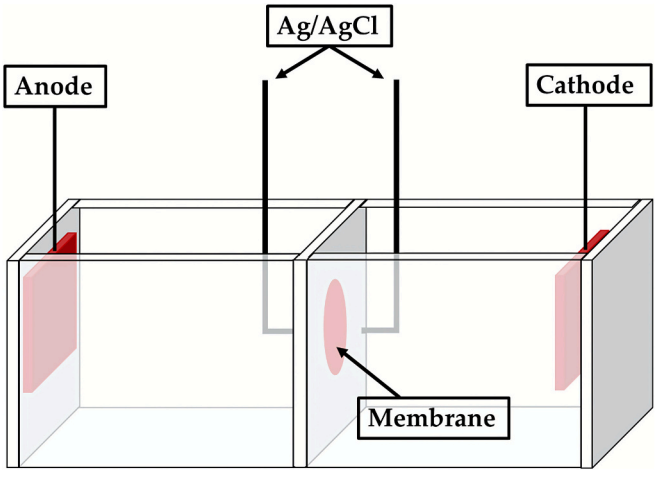

Fig. 2. Experimental setup for linear sweep voltammetry measurements.

hour during the first 5 h and after 24 h, to ensure the membranes were saturated. The water on the surface of the wet membranes was quickly removed with filter paper, and then the mass was measured. The mass of the dry membranes was obtained after drying them at 50 °C, until constant mass was reached. All experiments were made by triplicate. The water uptake was calculated as follows:

$$Water\ uptake\ (\%) = \frac{(Wwet - Wdry)}{Wdry} \cdot 100 \quad (1)$$

Where W_{wet} and W_{dry} are the mass of wet and dry membrane samples, respectively.

The same procedure was used to determine the methanol uptake. In these cases, 2, 6 and 12 M solutions of methanol in water were used. Measurements were taken every hour for the first 5 h, and after 24 h, to ensure complete methanol saturation of the membranes.

A Keyence digital microscope VHX – 7000 series with 4 K high-resolution camera was used to analyse the surface morphology of the prepared hybrid membranes.

3. Results and discussion

As previously described, we synthetized and characterized a family of side chain liquid crystalline poly(2-oxazoline)s from the dendritic monomer 2-(3,4,5-tris(4-dodecyloxybenzyloxy)phenyl)-4,5-dihydro-1,3-oxazole by cationic ring opening polymerization (CROP). XRD analysis confirmed that the presence of the dendritic moieties in the polymer structure allows the self-assembly of these poly(2-oxazoline)s into columnar structures [21].

3.1. Membrane preparation

For membrane preparation, we chose PTOx40 (DP = 40, Fig. 1), as it was the only polymer exhibiting a clear hexagonal columnar mesophase, as observed by DSC and XRD (**Fig. S1** and **Table S1**) [21]. Because the membranes prepared with PTOx40 were too brittle to be self-supported, a polyester fabric (Hollytex®, 22 g/cm^2) was used as a support for the preparation of hybrid membranes based on PTOx40 (**Fig. S2**). This nonwoven polyester fabric is lightweight and mechanically resistant, enhancing the processing of the PTOx40-based membranes by providing flexibility, reducing brittleness, and improving mechanical strength. To prepare the hybrid membranes, the polyester fabric was impregnated with a PTOx40 solution in THF, followed by polymer precipitation and air drying (Scheme 1).

As mentioned earlier, membranes prepared with columnar polymers require proper columnar alignment to function effectively as ion channels for cation transport. In our previous works, we reported the successful homeotropic orientation of various SCLC polyethers and polyamines by slowly cooling them from the molten state to room temperature [13–15,19,20]. However, different parameters can influence the final degree of orientation of the polymer chains, including annealing temperature, cooling rate, and annealing time [15]. In this study, we investigated two annealing temperatures, 69 and 73 °C. All prepared membranes were cooled down from the melt at 0.5 °C/min and subsequently annealed for 24 h.

Besides, we evaluated the effect of the support on which the membranes were prepared on the orientation of the polymer columns. Bogdanowicz and *co*-workers reported that using two different supports (hydrophilic treated glass or hydrophobic Teflon) did not produce significant differences in the orientation of the polymer chains [23]. Nevertheless, in this work, a more in-depth investigation was conducted by performing thermal treatment on hybrid membranes laminated onto supports with varying hydrophobic/hydrophilic properties. The supports used were untreated glass (hydrophilic), Fluorinated Ethylene Propylene Resin (FEPR) sheet (hydrophobic), and silanized glass (hydrophobic). Consequently, four different membranes were prepared: PTOxM-73-UG and PTOxM-69-UG (untreated glass), PTOxM-69-FEPR (FEPR sheet), and PTOxM-69-SG (silanized glass).

3.2. Structural and morphological characterization of the membranes

The PTOx40-based membranes were characterized by XRD to determine the organization of the polymer columns within Hollytex®. The diffractograms of the four distinct prepared membranes are shown in Fig. 3, and the corresponding XRD data are summarized in Table 1.

The reflection centered at $2\theta = 2.27°$, which is observed in all of them, confirmed the presence of columnar structures. This peak was assigned to the lattice plane (100), as reported in previous studies [12–14,18,19,21]. For PTOxM-73-UG, no narrow peak was observed in its azimuthal scan on the d_{100}. This indicates that no homeotropic orientation of the polymer columns was achieved when the annealing was carried out at 73 °C. This highlights the importance of the annealing temperature on the orientation of the polymer columns within the membrane. The higher mobility of the polymer columns at 73 °C may have hindered equilibrium during the 24-h annealing stage. As a result, annealing at this temperature did not yield the desired column organization. Longer annealing times were not tested at 73 °C, as previous work demonstrated that extending the annealing period did not improve column orientation [15]. In the azimuthal scans of the membranes annealed at 69 °C, the peak centered at $\phi = 270°$ observed for all membranes confirmed that the polymer columns were homeotropically oriented. This peak is relatively narrow for these three membranes, with the calculated width at half-height (WHH) ranging from 7.80° to 8.10°.

Moreover, comparison of the relative intensity of the peak centered at 270° in the azimuthal scans revealed that the membranes exhibited improved orientation when annealed on hydrophobic supports (FEPR sheet and silanized glass).

To examine the membrane surfaces, topographic analysis was performed using an optical microscope. This analysis allowed the identification of visible structural defects, such as surface discontinuities or cracks. As shown in Fig. 4, all prepared membranes exhibited homogeneous surfaces. The unoriented membrane, PTOxM-73-UG, exhibited the most irregular surface among the membranes analysed. In contrast, the oriented membranes exhibited a smoother, less wavy surface.

After detaching the membranes from the substrates, a similar analysis was performed on their bottom surfaces. As an example, **Fig. S3** shows the bottom surfaces of the PTOx40M-69-FEPR and PTOxM69-SG membranes. In both cases, the bottom surfaces exhibited a roughness similar to that of the air-facing sides.

Polyester fabric fibers were also analysed by optical microscopy to assess whether they were affected by impregnation with PTOx40. As shown in **Fig. S4**, no detectable differences were observed between the fibers before and after the preparation of the PTOx40-based membranes. It can be seen that in both cases, the polyester fabric fibers exhibited a similar thickness (25–35 μm). Therefore, impregnation of the Hollytex® support with PTOx40 did not cause fiber swelling but rather filled the voids between the fibers.

Furthermore, static water contact angle (CA) measurements were performed to assess the effect of column orientation on the membrane surfaces (Table 2). In previous studies, we observed an increase in CA values for the surfaces of thermally treated, self-supported membranes prepared from SCLC polyamines and polyethers bearing TAP side dendrons [13,18,24]. This phenomenon is associated with an increase in the hydrophobic character of the membrane, which we attributed to the homeotropic orientation of the polymer columns. After the homeotropic orientation, the TAP groups are more exposed at the surface while surrounding the polar polymer main chain.

Nonetheless, practically no differences were observed between the oriented and unoriented membranes of this family (Table 2). To clarify this result, CA measurements were also performed on the Hollytex® support. As shown in **Fig. S5**, the CA value of the polyester fabric was very similar to those obtained for the tested membranes. This indicates that the hydrophobic character of Hollytex® predominantly determines

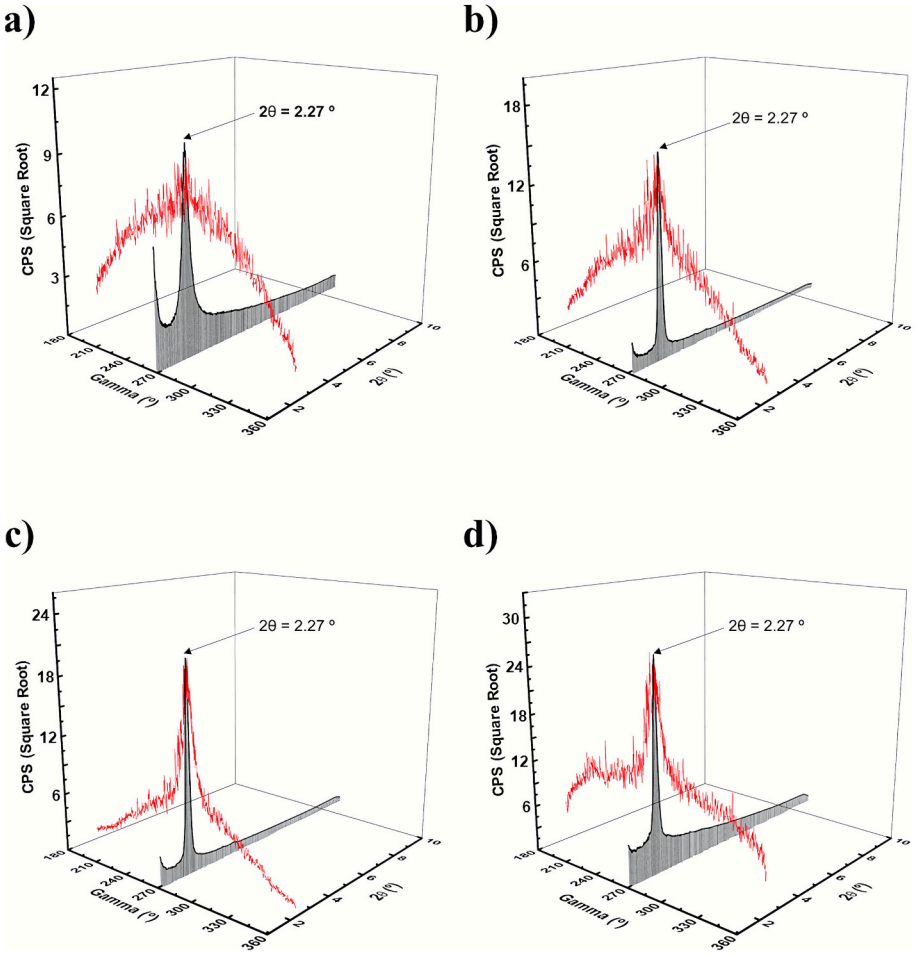

Fig. 3. X-ray diffractograms and the corresponding azimuthal scans, on the reflection (100), of the thermally treated hybrid membranes: a) PTOxM-73-UG, b) PTOxM-69-UG, c) PTOxM-69-FEPR, and d) PTOxM-69-SG.

Table 1
Annealing temperatures and XRD diffraction data of PTOx40-based membranes.

Membrane	Annealing temperature (°C)	Orientation	2θ (°)	d_{100} (Å)	Mesophase [a]	WHH (°) [b]	Angle of orientation (°)
PTOxM-73-UG	73	No orientation	2.27	38.6	*Col*	–	–
PTOxM-69-UG	69	Homeotropic	2.27	38.6	*Col*	7.80	270
PTOxM-69-FEPR	69	Homeotropic	2.27	38.6	*Col*	8.10	270
PTOxM-69-SG	69	Homeotropic	2.27	38.6	*Col*	7.80	270

[a] *Col*: columnar.
[b] WHH: width at half-height.

the measured CA of the membranes. Moreover, the TAP groups are directly grafted to the nitrogen atom of the poly(2-oxazoline) main chain, which limits their mobility. In contrast, in dendronized polymers reported in previous studies, a methyl or an ethyl spacer connected the polymer backbone to the TAP dendrons.

As mentioned above, the membranes were assembled over hydrophobic (untreated glass) or hydrophilic (FEPR sheet and silanized glass) substrates. As shown in Table 2, the CA values of the membrane bottom surfaces were similar, indicating that the nature of the substrate does not affect their wettability.

To evaluate the influence of the aqueous environment and methanol, uptake tests were conducted using both water and methanol aqueous solutions. The results showed almost identical behaviour for all membranes, regardless of their orientation, in both water and methanol solutions. Mass measurements over time indicated complete solution uptake within the first hour for all solutions and concentrations. As shown in Table 2, water uptake values remained consistently around 10% for all membranes, notably lower than values reported for Nafion® membranes [25]. Methanol uptake led to a weight increase of 4–8%. Besides, the membranes did not swell, making these hybrid membranes promising candidates for energy production systems where methanol serves as the fuel.

3.3. Ionic transport properties of the membranes

The ionic conductivity of oriented and unoriented hybrid membranes was initially investigated using electrochemical impedance spectroscopy (EIS). The Nyquist plots representing the EIS impedance analysis through-plane of all the dry membranes are shown in Fig. 5. The impedance results show lines that are practically straight along the y-axis, with impedance values approaching zero for all tested membranes, corresponding to high-frequency values (resistance values were on the

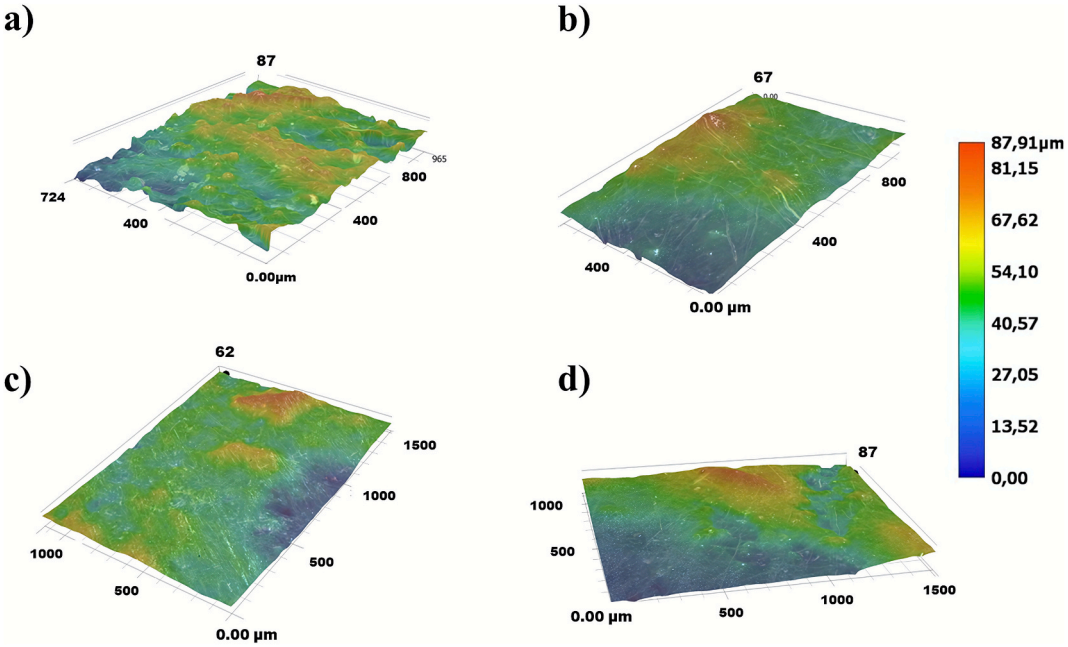

Fig. 4. 3D images of the top surface of the hybrid membranes: a) PTOxM-73-UG, b) PTOxM-69-UG, c) PTOxM-69-FEPR, and d) PTOxM-69-SG recorded with an optical microscope at RT (25 ± 5 °C).

Table 2
Water contact angles, water and methanol uptake after 24 h of Hollytex® (22 g/cm^2) polyester fabric support, unoriented (PTOxM-73-UG) and oriented (PTOxM-69-UG, PTOxM-69-FEPR and PTOxM-69-SG) membranes.

Membrane	Water contact angle (°)		Water uptake (%)[a]	Methanol uptake (%)[a]		
	Air side	Substrate side		2 M	6 M	12 M
Hollytex® (22 g/cm^2)	114 ± 1	–	23 ± 2	25 ± 1	26 ± 2	24 ± 2
PTOx40[b]	105 ± 1	–	–	–	–	–
PTOxM-73-UG	109 ± 1	111 ± 2	10 ± 1	4 ± 2	4 ± 2	5 ± 2
PTOxM-69-UG	113 ± 1	111 ± 2	11 ± 2	6 ± 1	5 ± 1	4 ± 1
PTOxM-69-FEPR	111 ± 2	117 ± 4	10 ± 1	8 ± 1	7 ± 2	4 ± 1
PTOxM-69-SG	112 ± 1	112 ± 2	10 ± 1	6 ± 1	4 ± 1	4 ± 1

[a] Water and methanol uptake after 24 h.
[b] PTOx40 polymer film on top of untreated glass without applying any thermal treatment.

order of 10^{11} Ω).

To describe the polymer conductivity behaviour of the hybrid membranes, we simulated the impedance data by fitting it to a simple electrical circuit model. These models were labelled using the "circuit description code" (CDC) [26]. In our cases, the observed Nyquist plots can be effectively modelled by an ideal capacitor (C). The corresponding equivalent circuit is shown in **Fig. S6**. This behaviour can be attributed to the non-ionic nature of the poly(2-oxazoline). Unlike Nafion®, which contains sulfonic acid groups that facilitate ionic conduction via polarizable ionic domains [27–30], the channels in the studied membranes lack ionic groups and are not pre-filled with mobile ions. In their pristine state, the membranes contain only weakly polarized bonds, resulting in high resistance values in EIS measurements. Consequently, the ionic conductivity cannot be directly inferred from EIS data.

In our systems, the membrane architecture was specifically designed

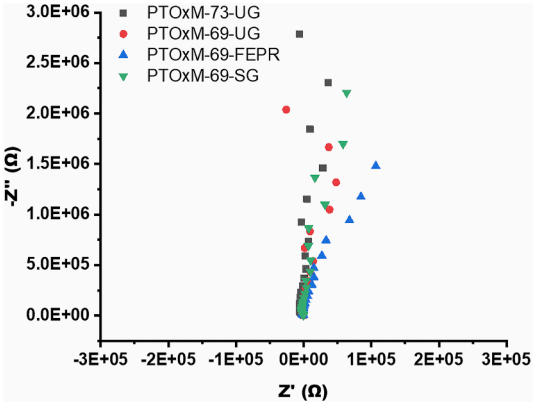

Fig. 5. Through-plane electrochemical impedance spectroscopy (EIS) Nyquist plots of dry hybrid membranes.

to enable cation solvation via the polymer backbone. It also promotes ionic transport under external stimuli, such as concentration gradients or applied electric fields. To evaluate the ionic conductivity of these hybrid membranes, alternative techniques, including permeability tests and linear sweep voltammetry, were employed.

Permeability tests on oriented membranes showed no pH change in the stripping solutions after 4 days, indicating negligible proton transport. These results differed from those previously reported for SCLC polyethers and polyamines [13,18,20]. The absence of proton transport in this SCLC poly(2-oxazoline), compared to polyamines or polyethers, can be attributed to the lower basicity and reduced mobility of the amide groups. These factors limit their ability to facilitate efficient proton hopping or coordination. Additionally, in PTOx40, TAP dendrons are directly grafted to the nitrogen atom of the poly(2-oxazoline) backbone, resulting in reduced dendron mobility. In contrast, flexible spacers were used in previous studies to connect the polymer main chain with the lateral mesogens, thereby enhancing chain orientation, and allowing proton transport [13,18,20].

To evaluate the ion transport properties, current-voltage (C—V) measurements were performed using the setup shown in Fig. 2. The

resulting C—V curves for the PTOx40-based membranes in 0.1 M HCl, which are shown in Fig. 6, exhibited three main characteristic regions. The first region (ohmic region) is observed at low voltages. In the ohmic region, a linear relationship between current and applied potential indicates ohmic or quasi-ohmic behaviour. The second region, also called limiting current region, is characterized by a plateau or semi-plateau that represents the maximum ion flux across the membrane. Besides, this region indicates cation permselectivity, where only cations significantly contribute to charge transport across the membrane. Finally, the third region, also called overlimiting region, is marked by a further increase in current, attributed to electroconvection or water dissociation phenomena [31–33]. The three characteristic regions for each curve are highlighted in **Fig. S7**.

In addition to proton conductivity, the transport of other alkaline monovalent cations (Li^+, Na^+, and K^+) was investigated. The results, summarized in Table 3 alongside the proton conductivity data, show that the unoriented PTOxM-73-UG membrane exhibited the highest R_{ohm} (1.111×10^7 [$\Omega \cdot cm^{-2}$]), up to two orders of magnitude greater than the other membranes tested in this work. It also showed a distinguishable limiting current region, consistent with the general behaviour observed for these hybrid membranes. For this unoriented membrane, the calculated limiting current (I_{lim}) density was the smallest one from

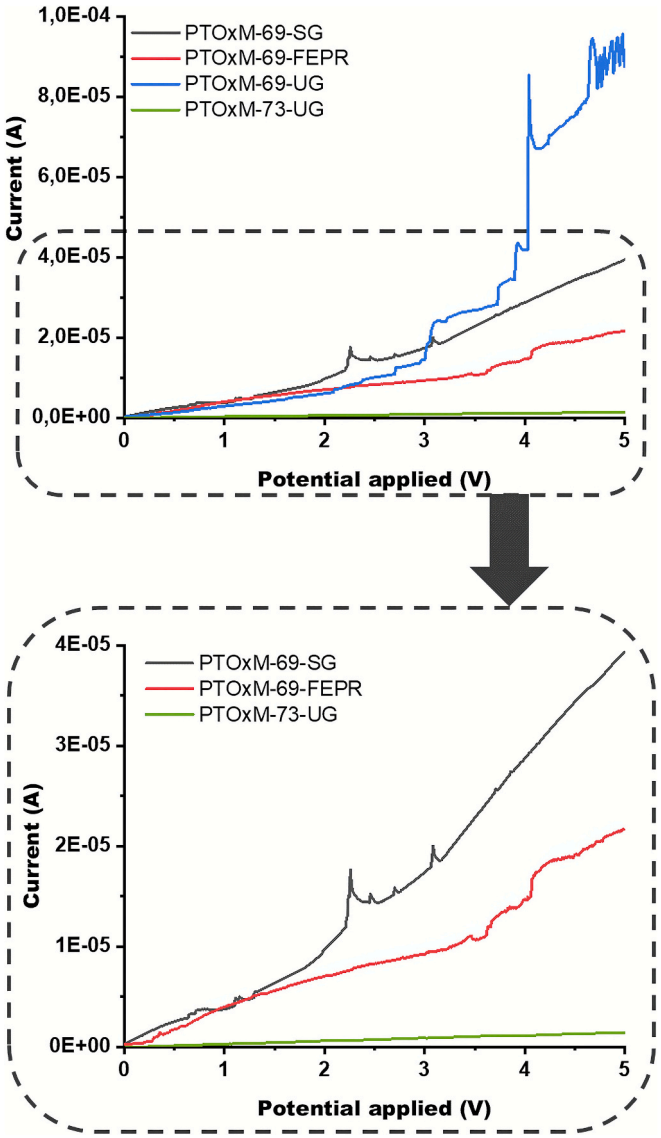

Fig. 6. C—V curves of PTOx40-based hybrid membranes.

Table 3
Ohmic resistances of the studied membranes obtained from C – V curves for the different cations.

Sample	R_{ohm} x 10^7 [$\Omega \cdot cm^{-2}$]			
	HCl	LiCl	NaCl	KCl
Nafion®117	0.003 [a]	0.006 [a]	0.019 [a]	0.012 [a]
PTOxM-73-UG	1.111	106.640	339.060	–
PTOxM-69-UG	0.082	17.630	125.860	311.312
PTOxM-69-FEPR	0.083	7.290	55.710	41.220
PTOxM-69-SG	0.084	7.141	147.824	279.544

[a] Ohmic resistance expressed in R_{ohm} x 10^3 [$\Omega \cdot cm^{-2}$]. Nafion® 117 ohmic resistances were reported by Bogdanowicz et al. [20].

this set of membranes ($I_{lim} = 2.27 \times 10^{-6}$ [$A \cdot cm^{-2}$]). The hybrid membrane PTOxM-69-UG exhibited an ohmic resistance (R_{ohm}) density of 0.082×10^7 [$\Omega \cdot cm^{-2}$]. The limiting current (I_{lim}) density of this membrane was greater than that of the unoriented membrane ($I_{lim} = 8.64 \times 10^{-5}$ [$A \cdot cm^{-2}$], but smaller than that of the membranes homeotropically oriented in hydrophobic supports (PTOxM-69-FEPR and PTOxM-69-SG). Regarding PTOxM-69-FEPR and PTOxM-69-SG, they showed similar R_{ohm} values (0.083 and 0.084×10^7 [$\Omega \cdot cm^{-2}$], respectively) with lower I_{lim} densities of 1.82×10^{-5} and 1.33×10^{-5} [$A \cdot cm^{-2}$], respectively.

The higher ohmic resistance density observed for unoriented PTOxM-73-UG membrane, compared to PTOxM-69-UG, PTOxM-69-FEPR, and PTOxM-69-SG, can be attributed to the lack of column orientation in the membrane structure of PTOxM-73-UG. This lack of orientation was confirmed by the azimuthal scan on the d_{100} reflection for PTOxM-73-UG, where a broad and low-intensity peak was observed (Fig. 3). Since PTOxM-73-UG was not oriented during preparation, the membrane exhibited poorly defined ion transport pathways, resulting in the highest resistance density value. Moreover, potassium ion transport was not detected in PTOxM-73-UG, making it impossible to determine its corresponding ohmic resistance density (Table 3). In contrast, PTOxM-69-FEPR and PTOxM-69-SG were assembled on hydrophobic substrates, which promoted better homeotropic column orientation, as evidenced by the intense peak centered at 270° in the azimuthal scan of these samples (Fig. 3). As a result of this orientation, these membranes exhibited lower resistance values. In the case of PTOxM-69-UG membrane, which was prepared on a hydrophilic substrate, it shows a certain homeotropic orientation since a peak centered at 270° is also observed in its azimuthal scan. However, the intensity of this peak is lower compared to the corresponding peak in the azimuthal scans of the two membranes prepared on hydrophobic substrates (PTOxM-69-FEPR and PTOxM-69-SG). This explains why the membrane PTOxM-69-UG showed slightly higher or comparable resistance to PTOxM-69-FEPR and PTOxM-69-SG, depending on the cation tested (H^+, Li^+, Na^+ and K^+). These findings demonstrate a direct correlation between membrane orientation, as revealed by XRD, and ionic transport performance, as seen in the C—V curves. Therefore, membranes exhibiting clear homeotropic column orientation show significantly lower ohmic resistance and higher limiting currents, whereas non-oriented membranes display markedly poorer transport properties.

In the LSV experiment, the potential difference between the electrodes first forces cations to overcome the interfacial barrier at the membrane-solution interface, followed by their transfer between the compartments. In some cases, the "filling of the membrane" is visible as a short plateau at the beginning of the C—V curves; however, possibly due to residual polarisation during membrane handling, this feature was not consistently observed for all membranes. During ion transport through an ionomeric membrane such as Nafion®, the ionic channels are already filled with cations, allowing cation flux without an initial filling stage [34,35].

Several models have been proposed to explain proton conductivity, including the Grotthus-Diffusion mechanism, the vehicular mechanism,

and others. The Grotthus-Diffusion mechanism occurs in the bulk phase, where excess protons move rapidly, by hopping through hydrogen-bonded water clusters. This mechanism requires a high degree of hydration and is typically observed only in swollen membrane pores. At low hydration levels, in the absence of bulk water, proton transport becomes dominated by a much slower surface-hopping mechanism, in which protons move from one sulfonic group to the next along the pore walls [34,36,37].

Studies on ion transport in non-ionomeric materials are relatively scarce in the literature; consequently, limited information is available on this topic. To properly understand the behaviour of non-ionomeric materials, several factors must be considered. In this work, the objective of minimizing the influence of water on membrane properties was achieved through the high hydrophobicity of the SCLC poly(2-oxazoline)s, which reduces membrane swelling and effectively excludes the Grotthus-Diffusion based transport mechanism. Other transport mechanisms, such as vehicular transport, are also expected to be strongly limited by the narrow channel size, which is primarily determined by the self-assembly process of the SCLC polymer chains and governs ion transport in these systems. Therefore, the most probable transport mechanism in these systems is proton hopping. This mechanism involves hydrogen bonding between the proton and the nitrogen atoms of the poly(2-oxazoline) main chain in the absence of bulk water molecules. Nevertheless, the aqueous environment likely facilitates cation transfer from the bulk solution to the membrane surface, and interactions between surface-bound water and the membrane may partly explain the observed water uptake of approximately 10%. This hopping-restricted transport mechanism could explain the low conductivity values observed for these SCLC poly(2-oxazoline)-based membranes. Importantly, compared to Grotthus-Diffusion and vehicular mechanisms, the proposed hopping-restricted transport mechanism offers the advantage of high cation selectivity, which is a key feature of the systems presented in this study.

An essential factor affecting the conductivity across the polymer columns formed by this type of SCLC polymers is the basicity of the heteroatom in the polymer main chain. In the case of SCLC poly(2-oxazoline)s and polyamines, this heteroatom is nitrogen. The nitrogen atoms exhibit lower basicity in SCLC poly(2-oxazoline)s compared with those in SCLC polyamines. Comparing the two systems, reducing the heteroatom's attractive force for the proton decreases the drag force across the polymeric channel responsible for proton transport. This may explain why the concentration gradient was ineffective in establishing a low potential difference between the two compartments for the SCLC poly(2-oxazoline)-based membranes, particularly when cation transport must occur simultaneously in both directions.

Regarding SCLC polyethers, although oxygen is expected to have lower basicity than nitrogen in SCLC polyamines, they exhibit proton conductivity similar to that of Nafion®, thanks to oxygen's ability to form hydrogen bonds [13]. Furthermore, the TAP side chain dendrons are grafted onto the SCLC polyamines and polyethers previously investigated by us via a flexible alkyl spacer [13,14]. This spacer is expected to increase the mobility of the TAP dendrons, influence the rearrangement of pendant TAP groups, and provide bypass pathways for protons due to the proximity of the carbonyl groups. Supporting this hypothesis, studies using Raman spectroscopy coupled with chronoamperometry on SCLC poly(epichlorohydrin-*co*-ethylene oxide) modified with TAP dendrons revealed that protons pass through the polyether backbone. Moreover, these experiments demonstrated that the lateral ester groups play an important role in cation transport, with the exception of sodium [38].

To evaluate the membranes' preferential selectivity for protons over the studied monovalent cations, the conductance ratio (reverse resistance) G_{ion}/G_{H+} was calculated for each membrane (Table 4). As shown by the calculated ratios, all membranes exhibit high proton selectivity. PTOxM-73-UG shows no selectivity for potassium cations, which is consistent with its lack of potassium transport.

Table 4
Selectivity (G_{ion}/G_{H+} ratio) values of studied membranes for alkaline monovalent cations.

Sample	G_{ion}/G_{H+} x 100 (%)		
	Li^+	Na^+	K^+
Nafion®117	47.30 [a]	14.20 [a]	22.80 [a]
PTOxM-73-UG	1.00	0.30	0.00
PTOxM-69-UG	0.50	0.07	0.03
PTOxM-69-FEPR	1.10	0.15	0.20
PTOxM-69-SG	1.20	0.06	0.03

[a] Nafion® 117 preferential selectivity data were reported by Bogdanowicz et al. [20].

The G_{ion}/G_{H+} values highlight the importance of homeotropic column orientation within the membrane structure, a key factor governing cation transport. Our results demonstrate that the studied membranes exhibit higher proton selectivity over monovalent cations such as Li^+, Na^+, and K^+, compared to those reported by Zare et al., who investigated the proton selectivity of membranes based on SCLC polyethers [18]. This difference may arise from structural factors. The membranes studied by Zare et al. featured tapered groups randomly distributed along the main chain through post-polymerization modification of the polyether. In contrast, our PTOx40-based membranes have a more uniform distribution of tapered groups, as each repeating unit of the SCLC poly(2-oxazoline) is grafted to a tapered mesogen. This distribution of TAP dendrons may reduce backbone flexibility and limit rearrangement, thereby facilitating proton transport while increasing resistance to larger cations. This hypothesis was demonstrated by our previous Raman investigations coupled with chronoamperometry on SCLC polyethers modified with TAP dendrons [38]. These results emphasize the importance of side dendron distribution and polymer backbone conformation in SCLCPs for promoting selective proton transport.

4. Conclusions

Hybrid membranes based on a SCLC poly(2-oxazoline) (PTOx40) supported on polyester fabric were systematically investigated to elucidate the interplay between structural organization, wettability, and ion transport. Thermal treatment successfully induced homeotropic orientation of the polymer columns. X-ray diffraction analysis revealed that hydrophobic substrates promoted better homeotropic orientation of the polymer columns compared to hydrophilic substrates. Wettability measurements indicated similar trends in water and methanol absorption across all membranes, with methanol uptake consistently lower than water uptake, suggesting potential applicability in methanol-mediated hydrogen systems. Static contact angle analysis confirmed the membranes' hydrophobicity, with values comparable to those of the polyester fabric support itself.

Ion transport properties were evaluated using electrochemical impedance spectroscopy (EIS), permeability tests and linear sweep voltammetry (LSV). EIS confirmed the non-ionic nature of the membranes, while permeability tests showed negligible transport of monovalent cations (Li^+, Na^+, and K^+), presumably due to spatial constraints within the polymer channels. In contrast, LSV measurements showed that homeotropically oriented membranes exhibited significantly lower resistance densities compared to unoriented counterparts, highlighting the importance of polymer column orientation in enhancing ion conduction. Although the absolute proton conductivity was lower than that of Nafion® 117, PTOx40-based membranes showed exceptional selectivity for protons over other monovalent cations. These findings position these hybrid membranes as promising candidates for selective proton transport in applications such as artificial photosynthesis and advanced energy conversion systems.

CRediT authorship contribution statement

Jordi Guardià: Writing – original draft, Methodology, Investigation, Formal analysis. **Krzysztof Artur Bogdanowicz:** Writing – review & editing, Validation, Supervision, Project administration, Formal analysis, Data curation, Conceptualization. **José Antonio Reina:** Writing – review & editing, Validation, Supervision, Resources, Project administration, Funding acquisition, Formal analysis, Data curation, Conceptualization. **Marta Giamberini:** Writing – review & editing, Supervision, Resources, Project administration, Funding acquisition. **Agnieszka Iwan:** Supervision, Resources, Project administration. **Xavier Montané:** Writing – review & editing, Validation, Supervision, Resources, Project administration, Funding acquisition, Formal analysis, Data curation, Conceptualization.

Declaration of competing interest

The authors declare that they have no known competing financial interests or personal relationships that could have appeared to influence the work reported in this paper.

Acknowledgements

This work was funded by the Spanish Research State Agency (Agencia Estatal de Investigación, AEI/ 10.13039/501100011033, grant number PID2020-116322RB-C32). The authors also thank the Universitat Rovira i Virgili and Diputació de Tarragona for a pre-doctoral contract (2020PMF-PIPF-21) within its Martí i Franquès programme. The authors also acknowledge Dr. Alex Fragoso for his help with LSV experiments, while also thanking to Dr. Francesc Gispert for his help in XRD experiments.

Appendix A. Supplementary data

Supplementary data to this article can be found online at https://doi.org/10.1016/j.reactfunctpolym.2026.106652.

Data availability

The raw data required to reproduce these findings cannot be shared at this time due to technical limitations, but supplementary information will be sent on request.

References

[1] D. Kweku, O. Bismark, A. Maxwell, K. Desmond, K. Danso, E. Oti-Mensah, A. Quachie, B. Adormaa, Greenhouse effect: greenhouse gases and their impact on global warming, J. Sci. Res. Rep. 17 (2018) 1–9, https://doi.org/10.9734/jsrr/2017/39630.
[2] M. Tanaka, Y. Takeda, T. Wakiya, Y. Wakamoto, K. Harigaya, T. Ito, T. Tarao, H. Kawakami, Acid-doped polymer nanofiber framework: three-dimensional proton conductive network for high-performance fuel cells, J. Power Sources 342 (2017) 125–134, https://doi.org/10.1016/j.jpowsour.2016.12.018.
[3] M. Pan, C. Pan, C. Li, J. Zhao, A review of membranes in proton exchange membrane fuel cells: transport phenomena, performance and durability, Renew. Sust. Energ. Rev. 141 (2021), https://doi.org/10.1016/j.rser.2021.110771.
[4] H. Zhang, P.K. Shen, Recent development of polymer electrolyte membranes for fuel cells, Chem. Rev. 112 (2012) 2780–2832, https://doi.org/10.1021/cr200035s.
[5] S. Wang, L. Shi, S. Zhang, H. Wang, B. Cheng, X. Zhuang, Z. Li, Proton-conducting amino acid-modified chitosan nanofibers for nanocomposite proton exchange membranes, Eur. Polym. J. 119 (2019) 327–334, https://doi.org/10.1016/j.eurpolymj.2019.07.041.
[6] B.R. Kaafarani, Discotic liquid crystals for opto-electronic applications, Chem. Mater. 23 (2011) 378–396, https://doi.org/10.1021/cm102117c.
[7] R.J. Carlton, J.T. Hunter, D.S. Miller, R. Abbasi, P.C. Mushenheim, L.N. Tan, N. L. Abbott, Chemical and biological sensing using liquid crystals, Liq. Cryst. Rev. 1 (2013) 29–51, https://doi.org/10.1080/21680396.2013.769310.
[8] M. Zhou, T.J. Kidd, R.D. Noble, D.L. Gin, Supported Lyotropic liquid-crystal polymer membranes: promising materials for molecular-size-selective aqueous nanofiltration, Adv. Mater. 17 (2005) 1850–1853, https://doi.org/10.1002/adma.200500444.
[9] T. Kato, M. Yoshio, T. Ichikawa, B. Soberats, H. Ohno, M. Funahashi, Transport of ions and electrons in nanostructured liquid crystals, Nat. Rev. Mater. 2 (2017), https://doi.org/10.1038/natrevmats.2017.1.
[10] Z.Z. Nie, B. Zuo, L. Liu, M. Wang, S. Huang, X.M. Chen, H. Yang, Nanoporous supramolecular liquid crystal polymeric material for specific and selective uptake of melamine, Macromolecules 53 (2020) 4204–4213, https://doi.org/10.1021/acs.macromol.0c00322.
[11] J. Guardià, J.A. Reina, M. Giamberini, X. Montané, An up-to-date overview of liquid crystals and liquid crystal polymers for different applications: a review, Polymers (Basel) 16 (2024) 2293, https://doi.org/10.3390/polym16162293.
[12] A. Šakalyte, J.A. Reina, M. Giamberini, Liquid crystalline polyamines containing side dendrons: toward the building of ion channels based on polyamines, Polymer (Guildf) 54 (2013) 5133–5140, https://doi.org/10.1016/j.polymer.2013.07.027.
[13] X. Montané, S.V. Bhosale, J.A. Reina, M. Giamberini, Columnar liquid crystalline polyglycidol derivatives: a novel alternative for proton-conducting membranes, Polymer (Guildf) 66 (2015) 100–109, https://doi.org/10.1016/j.polymer.2015.03.071.
[14] X. Montané, K.A. Bogdanowicz, G. Colace, J.A. Reina, P. Cerruti, A. Lederer, M. Giamberini, Advances in the design of self-supported ion-conducting membranes-new family of columnar liquid crystalline polyamines. Part 1: Copolymer synthesis and membrane preparation, Polymer (Guildf) 105 (2016) 298–309, https://doi.org/10.1016/j.polymer.2016.10.047.
[15] A. Zare, B. Pascual-Jose, S. De la Flor, A. Ribes-Greus, X. Montané, J.A. Reina, M. Giamberini, Membranes for cation transport based on dendronized poly (epichlorohydrin-co-ethylene oxide). Part 1: the effect of dendron amount and column orientation on copolymer mobility, Polymers (Basel) 13 (2021) 3532, https://doi.org/10.3390/polym13203532.
[16] V. Percec, M. Glodde, T.K. Bera, Y. Miura, I. Shiyanovskaya, K.D. Singer, V.S. K. Balagurusamy, P.A. Heiney, I. Schnell, A. Rapp, H.W. Spiess, S.D. Hudsonk, H. Duan, Self-organization of supramolecular helical dendrimers into complex electronic materials, Nature 417 (2002) 384–387, https://doi.org/10.1038/nature01072.
[17] A. Rapp, I. Schnell, D. Sebastiani, S.P. Brown, V. Percec, H.W. Spiess, Supramolecular assembly of dendritic polymers elucidated by ^{1}H and ^{13}C solid-state MAS NMR spectroscopy, J. Am. Chem. Soc. 125 (2003) 13284–13297, https://doi.org/10.1021/ja035127d.
[18] A. Zare, B. Pascual-Jose, S. De la Flor, A. Ribes-Greus, X. Montané, J.A. Reina, M. Giamberini, Membranes for cation transport based on Dendronized poly (epichlorohydrin-co-ethylene oxide). Part 2: membrane characterization and transport properties, Polymers (Basel) 13 (2021) 3915, https://doi.org/10.3390/polym13223915.
[19] K.A. Bogdanowicz, G.A. Rapsilber, J.A. Reina, M. Giamberini, Liquid crystalline polymeric wires for selective proton transport, part 1: wires preparation, Polymer (Guildf) 92 (2016) 50–57, https://doi.org/10.1016/j.polymer.2016.03.073.
[20] K.A. Bogdanowicz, P. Sistat, J.A. Reina, M. Giamberini, Liquid crystalline polymeric wires for selective proton transport, part 2: ion transport in solid-state, Polymer (Guildf) 92 (2016) 58–65, https://doi.org/10.1016/j.polymer.2016.03.080.
[21] J. Guardià, M. Giamberini, J.A. Reina, X. Montané, Synthesis and characterization of dendronized side chain liquid crystalline poly(2-oxazoline)s towards biomimetic ion channels, Eur. Polym. J. (2023) 112273, https://doi.org/10.1016/j.eurpolymj.2023.112273.
[22] D.D. Perrin, W.L.F. Armarego, Purification of Laboratory Chemicals, Pergamon Press, 2009.
[23] K.A. Bogdanowicz, S.V. Bhosale, Y. Li, I.F.J. Vankelecom, R. Garcia-Valls, J. A. Reina, M. Giamberini, Mimicking nature: biomimetic ionic channels, J. Membr. Sci. 509 (2016) 10–18, https://doi.org/10.1016/j.memsci.2016.02.038.
[24] X. Montané, K.A. Bogdanowicz, J. Prats-Reig, G. Colace, J.A. Reina, M. Giamberini, Advances in the design of self-supported ion-conducting membranes – new family of columnar liquid crystalline polyamines. Part 2: ion transport characterisation and comparison to hybrid membranes, Polymer (Guildf) 105 (2016) 234–242, https://doi.org/10.1016/j.polymer.2016.10.046.
[25] T.A. Zawodzinski, C. Derouin, S. Radzinski, R.J. Sherman, V.T. Smith, T. E. Springer, S. Gottesfeld, Water uptake by and transport through Nafion® 117 membranes, J. Electrochem. Soc. 140 (1993) 1041–1047, https://doi.org/10.1149/1.2056194.
[26] A.C. Lazanas, M.I. Prodromidis, Electrochemical impedance spectroscopy—A tutorial, ACS Measure. Sci. Au 3 (2023) 162–193, https://doi.org/10.1021/acsmeasuresciau.2c00070.
[27] M. Shabani, M.H. Entezari, Designing continuous proton-conductive channels for direct methanol fuel cell through the sulfonated poly(ether ether ketone)/carbon quantum dot/graphitic carbon nitride nanosheet, Eur. Polym. J. 202 (2024), https://doi.org/10.1016/j.eurpolymj.2023.112641.
[28] J.H. Lim, J. Hou, W.Y. Kim, S. Wi, C.H. Lee, The relationship between chemical structure of perfluorinated sulfonic acid ionomers and their membrane properties for PEMEC application, Int. J. Hydrog. Energy 49 (2024) 794–804, https://doi.org/10.1016/j.ijhydene.2023.09.131.
[29] M. Díaz, A. Ortiz, I. Ortiz, Progress in the use of ionic liquids as electrolyte membranes in fuel cells, J. Membr. Sci. 469 (2014) 379–396, https://doi.org/10.1016/j.memsci.2014.06.033.
[30] S. Tan, Y. Wu, T. Liang, X. Yang, Kinetic modeling of anhydrous proton conduction in side chain liquid crystal polyacrylates, Int. J. Hydrog. Energy 39 (2014) 17391–17397, https://doi.org/10.1016/j.ijhydene.2014.08.043.
[31] E.H. Rotta, M.C. Martí-Calatayud, V. Pérez-Herranz, A.M. Bernardes, Evaluation by means of electrochemical impedance spectroscopy of the transport of phosphate ions through a heterogeneous anion-exchange membrane at different pH and

electrolyte concentration, Water (Switzerland) 15 (2023), https://doi.org/10.3390/w15010009.
[32] J.H. Choi, J.S. Park, S.H. Moon, Direct measurement of concentration distribution within the boundary layer of an ion-exchange membrane, J. Colloid Interface Sci. 251 (2002) 311–317, https://doi.org/10.1006/jcis.2002.8407.
[33] J.H. Choi, H.J. Lee, S.H. Moon, Effects of electrolytes on the transport phenomena in a cation-exchange membrane, J. Colloid Interface Sci. 238 (2001) 188–195, https://doi.org/10.1006/jcis.2001.7510.
[34] C. Cosse, M. Schumann, D. Becker, D. Schulz, Simulation of electric field control effects on the ion transport in proton exchange membranes for applications in fuel cells and electrolysers, Int. J. Hydrog. Energy 47 (2022) 7961–7974, https://doi.org/10.1016/j.ijhydene.2021.12.116.
[35] Z. Cao, R. Kumar, Y. Peng, G.A. Voth, Proton transport under external applied voltage, J. Phys. Chem. B 118 (2014) 8090–8098, https://doi.org/10.1021/jp501130m.
[36] P. Choi, N.H. Jalani, R. Datta, Thermodynamics and proton transport in Nafion: II. Proton diffusion mechanisms and conductivity, J. Electrochem. Soc. 152 (2005) E123, https://doi.org/10.1149/1.1859814.
[37] S. Feng, G.A. Voth, Proton solvation and transport in hydrated Nafion, J. Phys. Chem. B 115 (2011) 5903–5912, https://doi.org/10.1021/jp2002194.
[38] K.A. Bogdanowicz, D. Pirone, J. Prats-Reig, V. Ambrogi, J.A. Reina, M. Giamberini, In situ raman spectroscopy as a tool for structural insight into cation non-ionomeric polymer interactions during ion transport, Polymers (Basel) 10 (2018), https://doi.org/10.3390/polym10040416.